Silver Recovery through a Fluoride Chemistry for Solar Module Recycling

by

Theresa Chen

A Thesis Presented in Partial Fulfillment
of the Requirements for the Degree
Master of Science

Approved December 2023 by the
Graduate Supervisory Committee:

Meng Tao, Chair
Michael Goryll
Shuguang Deng

ARIZONA STATE UNIVERSITY

May 2024

ABSTRACT

With the demand growing for more sustainable forms of energy in replacement of fossil fuels, a major obstacle arises in the end-of life solar modules that are disposed of in landfills. Aside from the hazardous materials, silicon solar modules contain valuable and scarce materials such as silver. Silver is used in many industries and many applications therefore the recycling and recovering of it is financially beneficial. The purpose of this research was to achieve high purity and recovery of silver using hydrofluoric acid.

The following work presents the feasibility of silver recovery through the process of leaching and electrowinning by examining the percent recovery and cathodic coulombic efficiency, followed by a chemical analysis to determine the purity. Varying conditions in leaching and electrowinning parameters are conducted in a synthetic solution to determine the effect on silver recovery and cathodic coulombic efficiency. It was determined that the silver recovery was dependent on the applied potential, system configuration and time. The system is capable of recovery rates of over 95% at -1 V. The system is further tested on solar cells to prove that silver can be recovered. There was over 99% purity from the experiments conducted in synthetic solution and from solar cells. Additionally, a circular chemistry is proposed that allows the reuse of hydrofluoric acid for leaching and electrowinning.

ACKNOWLEDGEMENTS

I would like to thank my principal investigator, Dr. Meng Tao for his support and guidance throughout my research. His insight, dedication and commitment to the project has given me an opportunity to expand my knowledge in a different field.

I would like to thank Dr. Michael Goryll and Dr. Shuguang Deng for their willingness to serve on my committee.

I would like to thank the students of Dr. Tao's group – Randy Adcock, Natalie Click, Dustin Nguyen, Kelvin Tan, Mao-Feng Tseng, and Tayyab Zubair for their companionship and support. Especially on the chemical side for our buddy system, their guidance, discussions, and chemical analyses that were performed.

Lastly, I would like to give appreciation to the staff of EHS for their knowledge and commitment to making sure that hazardous waste is disposed of properly.

The research was made possible by the support of the US Department of Energy through the REMADE Institute, grant no. 21-01-RR-5014.

TABLE OF CONTENTS

Page

CHAPTER Page

LIST OF TABLES

Table Page

LIST OF FIGURES

Figure Page

CHAPTER 1 INTRODUCTION

1.1 Overview

Solar energy is efficient, clean and the third most used renewable energy source after hydro and wind power, respectively [1]. This in turn causes photovoltaic (PV) technology to contribute a vital role in fulfilling non-fossil fuel energy needs over recent decades and its ability to continue doing so. Solar panels currently have a lifespan of 30-35 years indicating these will be a pressing issue for the next decades as they will be disposed of in a landfill [2]. In 2035, it is predicted that approximately one million tonnes of solar modules will be discarded [3] and by 2050, between 60 and 78 million tonnes of PV waste in circulation [4]. This combined with the scarcity in metals [5] leads to a challenge of a demand in raw materials and the need of recycling solar modules. Raw materials recoverable from PV panels could yield a value of up to USD 450 million by 2030 and equate to approximately 60 million new panels or 18 GW of power-generation capacity [6].

As of July 2012, the European Union revised the waste electrical and electronic equipment (WEEE) directive, adding PV components as part of it [6]. However, aside from the EU, there are very few countries acting on end-of-life solar module recycling it due to its low cost-benefits [6]. Furthermore, EOL photovoltaic panel processing and recycling facilities are scarce around the world. This suggests that the end-of-life solar module recycling is a field that needs more research. With rising concern over disposing

these modules in landfill due to their environmental impact and regulations placed on certain materials (i.e. lead) [6], an appropriate recycling EOL management is necessary as these panels are becoming an issue with the continued number of installations.

Most of the market share is made up of crystalline silicon (c-Si) solar modules. The components of a c-Si module are displayed in Figure 1-1, the major components that make it up include an aluminum frame that protects the internal components and glass that protects the cell [8]. The internal components include (from top to bottom) – polymeric encapsulant, silicon solar cell, polymeric encapsulant and backsheet. The encapsulating material is generally ethylene vinyl acetate (EVA) that helps adhere the solar cell to the glass and backsheet [8]. The backsheet can range from polymer materials mainly consisting of fluorinated polymers such as polyvinyl fluoride, polyvinylidene fluoride or polyvinylidene fluoride [8]. Indicated on the right of the figure is the solar cell with the silver stripes for conductivity and soldered with copper busbars that interconnect the single cells within the module [9].

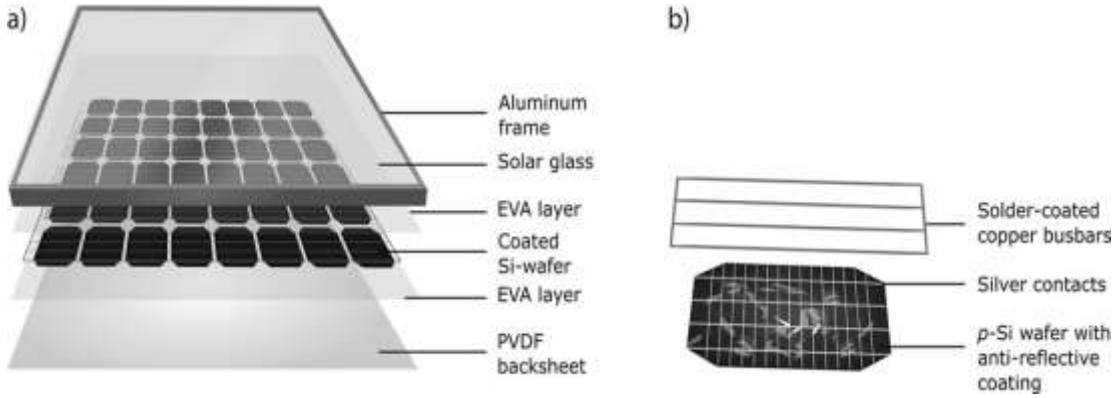

Figure 1-1: Component of a) Photovoltaic Module with the Layers Signified and b) Silicon Wafer Magnified to Show a Single Cell and the Layout and its Counterparts [9]

To break down the components involved, Table 1.1 indicates the components and chemical compositions seen in a solar module (these values may differ slightly depending on the supplier and manufacturing company).

Table 1.1: Composition and Components of C-Si Modules by Weight Percent [10]

Material	Weight (%)
Glass	74
Aluminum	10
Silicon	~3
Polymers	~6.5
Tin	0.12
Lead	<0.1
Copper	0.6
Silver	<0.006

Although the glass and aluminum make up more than 80% in mass in a silicon module, two-thirds of the monetary value is from the solar cells' individual components such as silver, silicon, and tin [11].

1.2 Objective

Hydrofluoric acid is proposed for silver recovery from silicon solar cells using a catalyst. It requires only two chemicals: hydrofluoric acid (HF) and hydrogen peroxide (H_2O_2), and two room-temperature steps: leaching and electrowinning. The goal of this was to end up with a high recovery and purity of silver while being able to recover other

components in the solar cell such as lead, tin, copper, and silicon. A sequential leaching and electrowinning process would be conducted to extract the metals and recover them. HF was chosen as a circular chemistry was proposed, this allows the acid to be reused in upcoming leaching and electrowinning processes.

1.3 Background

For metal extraction, the two most common types are pyrometallurgy and hydrometallurgy processes [12]. The chemistry of silver and HF utilizes the hydrometallurgy process. This involves the use of aqueous chemistry for the recovery of metals from ores, concentrates, and recycled or residual materials [13]. This route is more advantageous as it is more predictable, uses lower temperatures and investment for implementation [14]. It can be divided into 3 general areas: (1) leaching, (2) solution concentration and purification, and (3) metal recovery.

1.3.1 General Concepts and Equations

Leaching refers to the process in which extraction of substances from solids is achieved from the dissolution in liquid [14]. In a leaching process, the oxidation potential, temperature, and pH solutions are often parameters that are manipulated to optimize dissolution of the metal [12].

The leaching process can be categorized into: (1) change of phase of the solute as it dissolves into the solvent, (2) diffusion through the solvent in the pores of the solid to the outside of the particle and (3) transfer of the solute from the solution in contact with the

particles to bulk of the solution [15]. For the rate of dissolution, the particle size, solvent, temperature, and agitation rate are some factors to consider. Smaller particle sizes lead to greater interfacial area between the solid and liquid, allowing higher rate of material transfer [15]. However, too small of a size may lead to wedges in the interstices of larger particles and impede the flow of the solvent [15]. The solvent should have low viscosity to allow free flow [15]. The temperature increases the diffusion coefficient, improving the rate of dissolution. Agitating the solvent will increase eddy diffusion and decrease sedimentation [15]. These relationships depend on various factors, solute, and solvent involved.

Generally, mass transfer in leaching solutions can be approximated by assuming a thin film that takes the place of the resistance to transfer. The equation of the mass transfer can be written as [15]:

$$\frac{dM}{dt} = \frac{k'A(c_S - c)}{b} \quad (1)$$

Where A is the area of the solid-liquid interface, b is the thickness of the film surrounding the particles, c is the concentration of the solute in the bulk solution at time t, c_s is the concentration of the saturated solution in contact with the particles, M is the mass of solute transferred in time and k' is the diffusion coefficient.

Electrowinning is defined as the cathodic deposition of a metal by the passage of an electric current using an insoluble anode [16]. An electrolytic process is created from an electrolyte (cations and anions) dissolved in water or polar solvents. When a voltage is

applied to the solution, the cations move towards the cathode, while the anions move towards the anode [17]. This is a basic principle on how electrowinning is conducted.

In three-electrode electrochemical systems, there consists of a working, counter, and reference electrode. The working electrode (WE) is where the chemistry of interest occurs [18]. The counter electrode (CE) completes the circuit of charge flow and maintains constant interfacial potential [18]. It allows the current to pass and will adjust potentials to balance the current observed at the working electrode [18]. The reference electrode (RE) measures and controls the working electrode potential without passing any current [18]. Common choices for a reference electrode include silver- silver chloride, mercury- mercurous sulfate, or saturated calomel electrode. Additionally, the electrolyte (in which the ions move through) is a liquid dissolved with salts or acids [19].

The applied potential is measured between the working and reference electrode. By driving the WE to more negative potentials, the energy of the electrons is raised [18]. The flow of electrons from electrode to solution creates a reduction current [18]. Similarly, the opposite will occur when a more positive potential is applied. The flow from the electrons from solution to electrode will create an oxidation current [18]. The movement of material from one place to another arises from the differences in electrical or chemical potential at two different locations through these mass transport types: migration, diffusion, and convection.

Figure 1-2 [20] displays the mechanics and location of their occurrence. A typical cell is divided by the bulk solution (far from electrode) and diffusion layer. The diffusion layer

assumes a stagnant layer that exists at the electrode surface where the concentration near the electrode is different than the bulk [18]. In the case of an excess of supporting electrolyte, migration is not important making the rate of mass transfer proportional to the concentration gradient at the electrode surface [18]. Migration carries the current in the bulk solution during electrolysis while diffusional transport occurs near the electrodes due to concentration gradients [18]. Near the electrode surface both diffusion and migration occur where the flux of the electroactive substance at the surface controls the rate of reaction and the faradaic current flowing in the circuit [18].

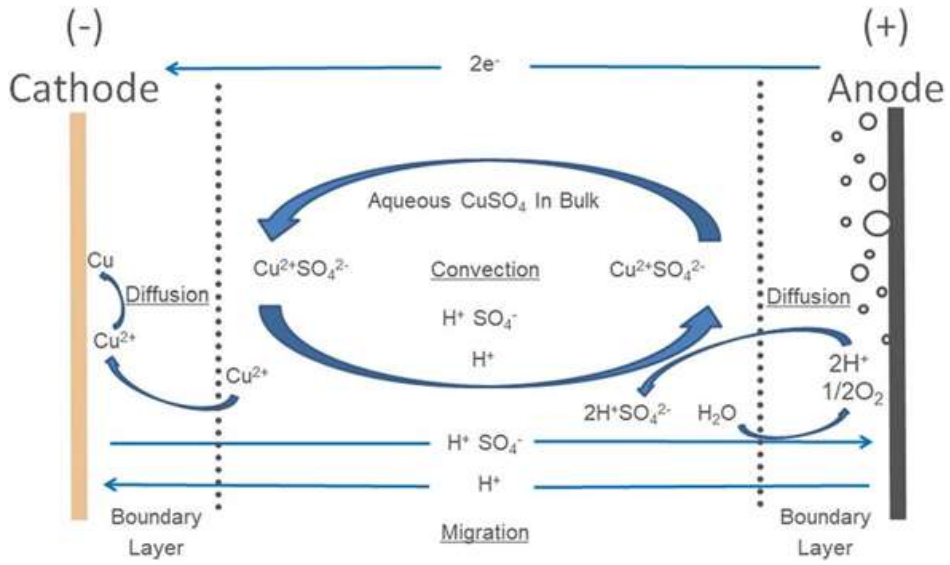

Figure 1-2: Cu Electrowinning in $CuSO_4$ Electrolyte Showing Bulk Solution and Boundary Layer [20]

Cyclic voltammetry is an electrochemical technique commonly used to determine reduction and oxidation processes [21]. It measures current that develops in an electrochemical cell where voltage is in excess [22]. This is governed by the Nerst equation [21],

$$E = E^{\circ} + 2.3026\frac{RT}{nF}log\frac{(Ox)}{(Red)} \quad (2)$$

Where E is the electrochemical cell potential, E° is the standard potential of a species, R is the universal gas constant, T is the temperature, n is the number of electrons, F is Faraday's constant, Ox is the activity of the oxidized analyte, and Red is the activity of the reduced analyte.

The equilibrium potential, E° is an important reference point in a system. The departure from E° is measured by the overpotential, η

$$\eta = E - E_{eq} \quad (3)$$

Where E is the potential of an electrode vs. RE and E_{eq} is the equilibrium potential. The overpotential (or underpotential) represents the extra energy needed to drive a reaction at a specific current density [18]. The magnitude of this value is dependent on the cell design, electrode shape and size, electrolyte composition and concentration, current density, etc [19].

Chronoamperometry was employed during silver electrowinning at a fixed constant potential. A general process is as follows [19]:

1) Mass transport of the reactant from the electrolyte to the electrode surface.
2) Surface interactions preceding electron transfer including the rearrangements of the deposited molecules, adsorption to the electrode surface, chemical reactions (protonation or disassociation).

3) Electron transfer at the cathode surface.
4) Surface conversion such as chemical reactions, desorption, insertion of metal cations into the crystal lattice.
5) Mass transport of the product from the electrode surface to the bulk electrolyte.

These experiments are common for studying the steady state performance of an electrode [22]. The potential applied is important in controlling the direction and rate of charge transfer [19]. The changes in the current arise from increases or decreases in the diffusion layer of the analyte near the surface of the cathode [23]. The optimal applied potential allows the local concentration to be zero. This allows a concentration gradient to drive the deposition [23].

The table illustrates that the larger the reduction potential, there is a greater tendency for the species to get reduced.

Table 1.2: Metal Reduction Potentials [24]

Metal	Reduction Reaction	E° vs SHE (v)
Ag	$Ag^{+} + e^{-} \leftrightarrow Ag$	0.7996
Cu	$Cu^{2+} + 2\ e^{-} \leftrightarrow Cu$	0.3419
Pb	$Pb^{2+} + e^{-} \leftrightarrow Pb$	-0.1262
Sn	$Sn^{2+} + 2e^{-} \leftrightarrow Sn$	-0.1375
Al	$Al^{3+} + 3e^{-} \leftrightarrow Al$	-1.662

1.3.2 Silver Properties

Silver is known as a ductile and malleable metal with a high electrical conductivity and low reactivity. Additionally, being an inactive metal, it does not react with oxygen in the air, acids, water, or other compounds under normal conditions. It has a high melting point of 961℃ and a density of 10.49 g/cm^3 at 20℃ [25]. It is extracted from lead-zinc, copper, gold, and copper-nickel ores as a byproduct of mining [25]. It exists in the +1, +2, and +3 oxidation state with +1 being the most common state. In comparison to the other metals in solar cells, it has a low reactivity. This indicates that it does not spontaneously react with acids or water.

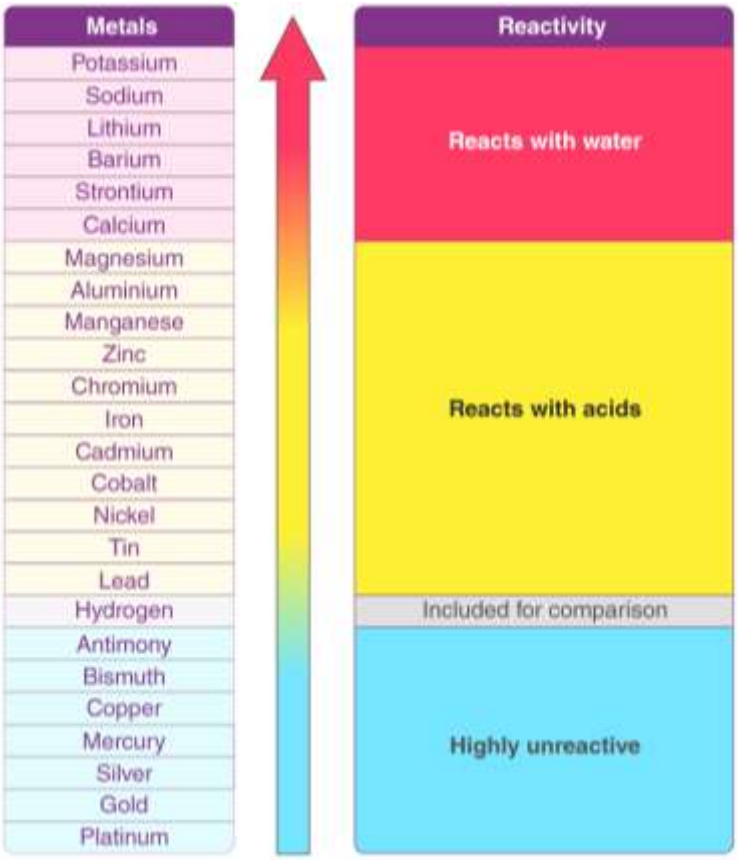

Figure 1-3: Reactivity Series [26]

1.3.3 HF Properties, Safety, and Hazards

Hydrofluoric acid is a colorless weak acid [27]. Due to the strong bond between the H and F molecules, it does not dissociate easily in water.

Table 1.3: Hydrofluoric Acid Physical Properties [27]

Molecular weight (g/mol)	20
Density (48% sol, g/mL)	1.23
Acidity (pKa)	3.17
Boiling point (°C)	66.4
Vapor pressure (kPa at 25°C)	122

HF is highly toxic and reactive to skin and tissue [27]. The seriousness of poisoning is dependent on the amount, route, length of exposure, age and preexisting medical condition of the person [27]. HF gas at low levels can irritate the eyes, nose, and respiratory tract. Low concentrations of HF on the skin may not be immediately visible or experienced. Prolonged exposure can cause persistent pain, bone loss and could be fatal [28]. It is crucial that personnel handling HF be aware of the precautions, proper equipment, and steps to take if HF is exposed through inhalation, ingestion, or skin contact.

1.4 Literature Review

A froth flotation process is employed for silver that is extracted from ores. The crushed ore is placed into a bath and silver is separated using air bubbles. The silver-rich froth is skimmed from the bath as represented from the diagram below [29]. Following the process, silver is smelted and extracted by cyanidation [30]. These processes not only

involve high temperatures, but sodium cyanide has an increased risk of explosions, release of toxic fumes and poses significant human health and aquatic hazards [31].

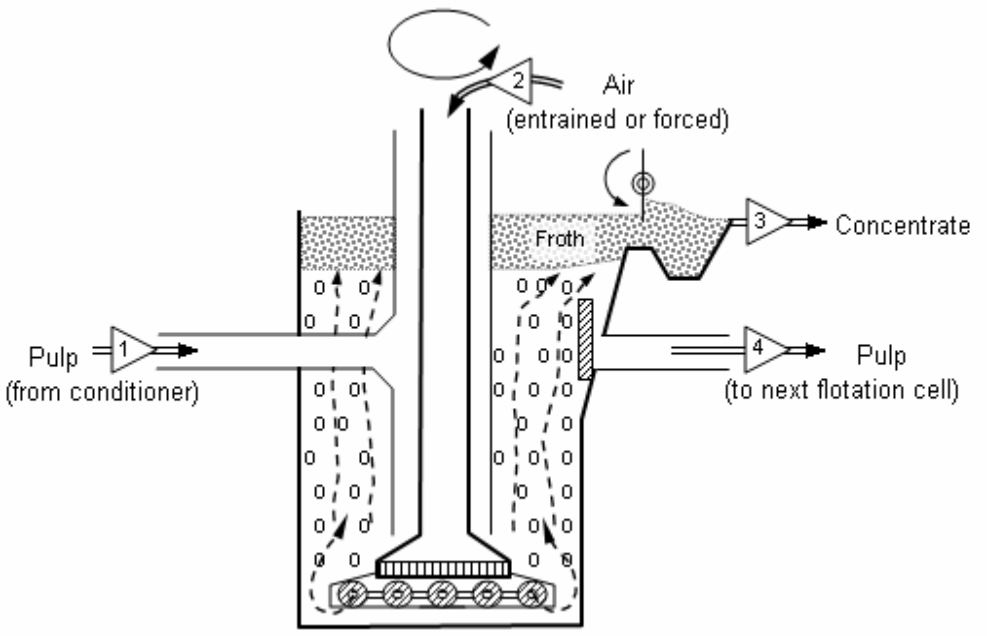

Figure 1-4: Froth Flotation Process [29]

Reports have indicated that the most notable silver recovery is with nitric acid (HNO_3). Dias et al. proposes the use of 64% nitric acid with 99% sodium chloride [31]. Parts of the PV module was immersed into sulfuric acid with agitation, filtered, rinsed, dried, and milled, respectively. Sieving was conducted that separated 0.5 mm silver particle sizes. Leaching was conducted using nitric acid for 2 hours at room temperature. Next, sodium chloride was added to the leached solution to form a silver chloride precipitate.

Another report by Oliveira et al. [33] leaches silver in nitric acid at temperatures of 25-60°C. For leaching the solid-liquid ratio used was 0.05 g/mL with optimal conditions of 2.3M HNO_3 at 55°C. Silver recovery was trialed by these 3 separate methods: chemical

precipitation with sodium carbonate, hydrochloric acid, or electrochemical precipitation. The conditions for the electrochemical process involved a steel working electrode and platinum counter electrode at room temperature. Sodium carbonate did not prove a suitable reagent as it resulted in low silver recovery (48%). Whereas hydrochloric acid and electro precipitation had high recoveries. Between the two, electro precipitation was chosen as there was less lead contamination.

Yang et al. [34] proposes the use of methanesulfonic acid (MSA) for the leaching of solar cells at varying ratios of MSA:H_2O_2 for 1-12 hours. Hydrochloric acid is added to the leached solution to precipitate silver chloride (AgCl) and centrifuged to separate the liquid and solid components. To convert AgCl, it is reacted with sodium hydroxide then hydrogen peroxide to recover silver powder. Further electrorefining was completed to improve the purity of the silver. Elements such as Ag, O, Al, Sn and Pb were present in the silver ingot.

CHAPTER 2 EXPERIMENTAL PROCEDURES

The following chemicals were used in this study: silver wire, silver fluoride (AgF), hydrogen peroxide (H_2O_2), hydrofluoric acid (HF), and sodium hydroxide (NaOH). All leaching and electrowinning experiments were conducted in open air at room temperature.

2.1 Silver Wire Leaching

Leaching experiments were conducted to determine the optimum conditions for silver dissolution. The mechanism of the chemical reaction is as follows:

$$2Ag + H_2O_2 \rightarrow Ag_2O + H_2O$$

$$Ag_2O + 2HF \rightarrow 2AgF + H_2O$$

$$2HF + 2Ag + H_2O_2 \rightarrow 2AgF + 2H_2O$$

1 gram of Ag wire was placed into 40 mL of 0.575 M HF solution and dissolved with the addition of H_2O_2 in a 1:2 Ag to H_2O_2 molar ratio. Additional experiments were conducted with the same conditions but varying the Ag to H_2O_2 molar ratio.

2.2 Cyclic Voltammogram

For cyclic voltammetry, a 0.05 M silver fluoride (AgF) solution was prepared to determine the reduction potential of silver. 0.0508 g of AgF was dissolved in 40 mL of 0.5 wt% HF (0.28 M) solution. The working and counter electrodes were both graphite rods. The reference electrode was a silver/silver chloride (Ag/AgCl) electrode from

EDAQ. The voltametric scans were generated with a Gamry Reference 3000 potentiostat at a scan rate of 100 mV/s.

2.3 Synthetic Electrowinning

Electrowinning experiments were carried out to determine the silver recovery rate and coulombic efficiency of the electrowinning process at various potentials and time intervals. The experiments for varying reduction potentials were in solutions of 0.5074 g of AgF (0.1 M) in 0.28 M HF for 4 hours (h). The potential which yielded the highest recovery rate was then used for the varying time intervals. The experiments for different time intervals were in solutions of 1.46 g of AgF (0.28M) in 0.28 M HF. For both groups of experiments, graphite rods were used as the working and counter electrodes with an Ag/AgCl reference electrode. This is displayed in Figure 2-1.

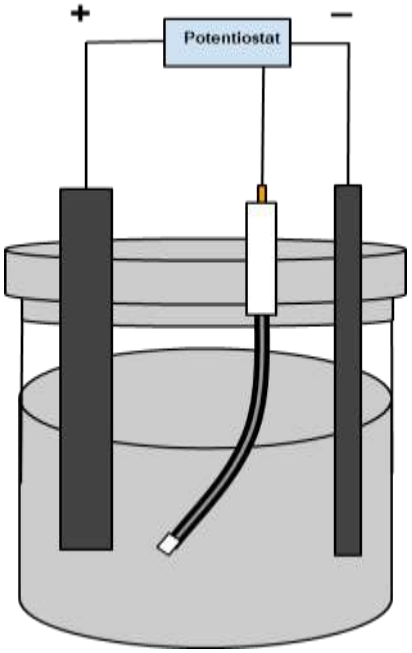

Figure 2-1: Electrowinning Setup

Where the following reactions are possible at the cathode and anode,

$$Cathode\ Ag^{+}(aq) + e^{-} \leftrightarrow Ag(s)$$

$$Anode\ 2H_2O\ (l) \leftrightarrow\ O_2(g) + 4e^{-} + 4H^{+}$$

2.4 Solar Cell Leaching and Electrowinning

Aluminum back surface field (Al-BSF) cells without the EVA and back sheet were crushed in a 121 x 121 mesh size polypropylene mesh. Leaching was conducted in the following order: aluminum, silicon nitride (Si-N_x) layer, and silver front and back contacts using 15 wt% sodium hydroxide, 1% HF and 1% HF plus hydrogen peroxide, respectively. Each of these steps were conducted with 400 mL of solution and disposed of for each step. For the silver front and back contacts, electrowinning was conducted at this

stage. The experiment was run in a scaled-up apparatus using 10 Al-BSF cells with 400 mL of solution at -1 V for 24 hours.

A JEOL JXA-8530 scanning electron microscope (SEM) equipped with an energy-dispersive spectrometer (EDS) was used to characterize the morphology and determine the elemental composition of the cathode deposit after electrowinning.

CHAPTER 3 RESULTS AND DISCUSSION

3.1 Silver Wire Leaching

Figure 3-1 displays the amount of Ag dissolved as a function of time. The solution contained 1 wt% HF and 1.86 mL of H_2O_2. The 1 g Ag wire was taken out of the solution every 10 minutes to measure the remaining weight. Ag dissolution starts increasing rapidly and plateaus after 30 minutes. The percentage dissolved at 30 minutes was 93% and complete dissolution was achieved within 1 hour. This trend follows what would be expected if there is a surplus of HF and hydrogen peroxide that allows the reaction to occur. It was observed that over time a thin white layer forms around the silver wire. At the point in which silver oxide forms and continues to develop over the wire, the dissolution rate increases. The silver oxide facilitates the dissolution of silver into the solution.

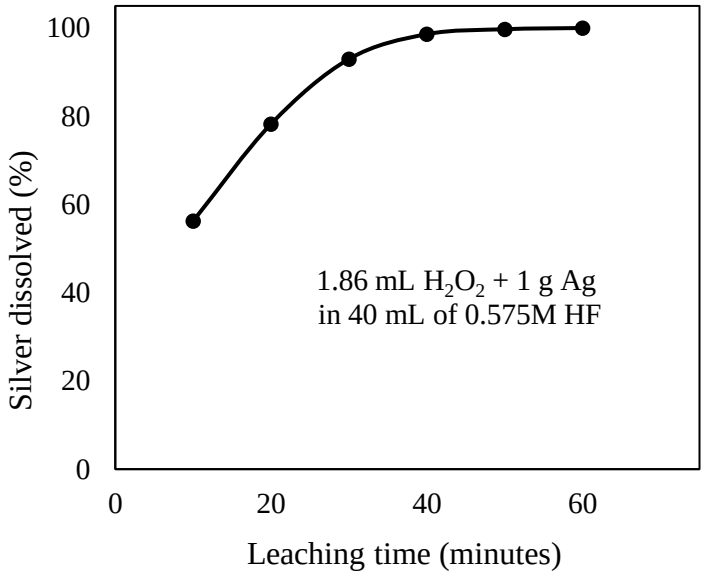

Figure 3-1: Percent Ag Leached as a Function of Time in 1 wt% With 1.86 mL H_2O_2 and 1 g of Ag Wire

Another parameter tested was the amount of H_2O_2 added to the leaching solution. The amount of hydrogen peroxide was varied to determine the amount that was needed for full dissolution of Ag. The range tested was 0.8 mL to 2 mL of H_2O_2 in increments of 0.25 mL. The leaching time was fixed at 1 hour. This study is presented in Figure 3-2. Except for the outlier at 1.35 mL, there is a clear trend − more H_2O_2 improved the percent of Ag dissolved. At 0.8 mL of H_2O_2, only 63% of the Ag is dissolved. With 2 mL of hydrogen peroxide, Ag dissolution reached 100%. These tests were done to replicate each experiment under the same conditions of silver amount, concentration, and volume of HF. A secondary set of tests were performed at 1.35 mL and 1.6 mL to confirm if the trend was due to experimental or human error. There is no change in the trend at these two data sets when varying hydrogen peroxide amounts were added.

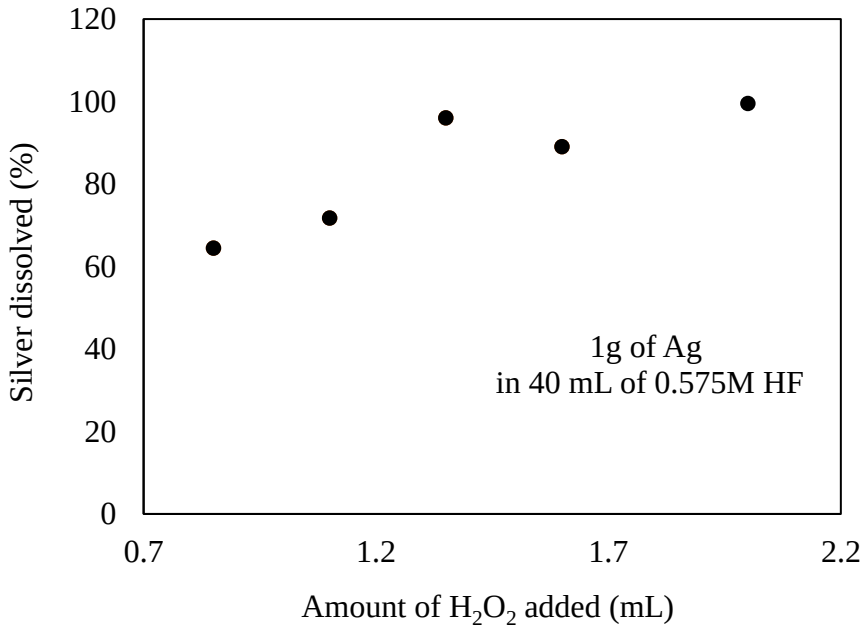

Figure 3-2: Percent Ag Leached as a Function of H_2O_2 Concentration in 1 wt% HF and 1 g of Ag for 1 Hour

3.2 Synthetic Electrowinning

Cyclic voltametric scans were generated to determine the reduction potential for Ag electrowinning. As shown in Figure 3-3, the blue lines represent a solution with only HF and the red line is a solution with both AgF and HF. The solution with 0.05 M AgF shows a clear reduction peak around -0.41 V versus an Ag/AgCl reference electrode. Additionally, there are no other peaks between -0.41 V and -1 V, suggesting that Ag electrowinning can be done up to -1 V without other reactions occurring.

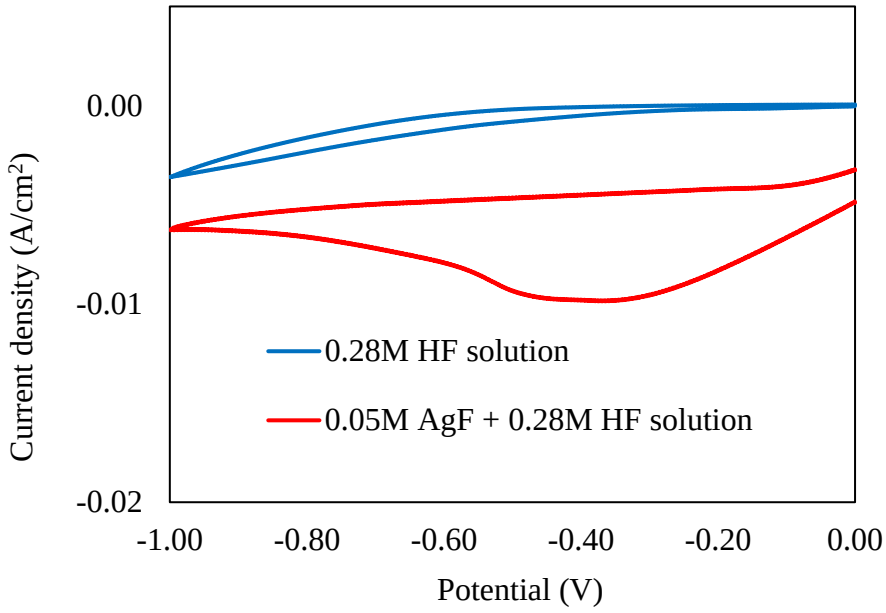

Figure 3-3: Cyclic Voltametric Scan of Solution of 0.05 M AgF + 0.28 M HF And 0.28 M HF Only

An EDS analysis was conducted on the deposit removed from the working electrode for 6 h of electrowinning. Figure 3-4 shows an SEM image of the morphology of the Ag recovered. Five points were chosen from the sample to determine the elemental

composition by EDS. The results indicate that the deposit on the working electrode is 100% Ag.

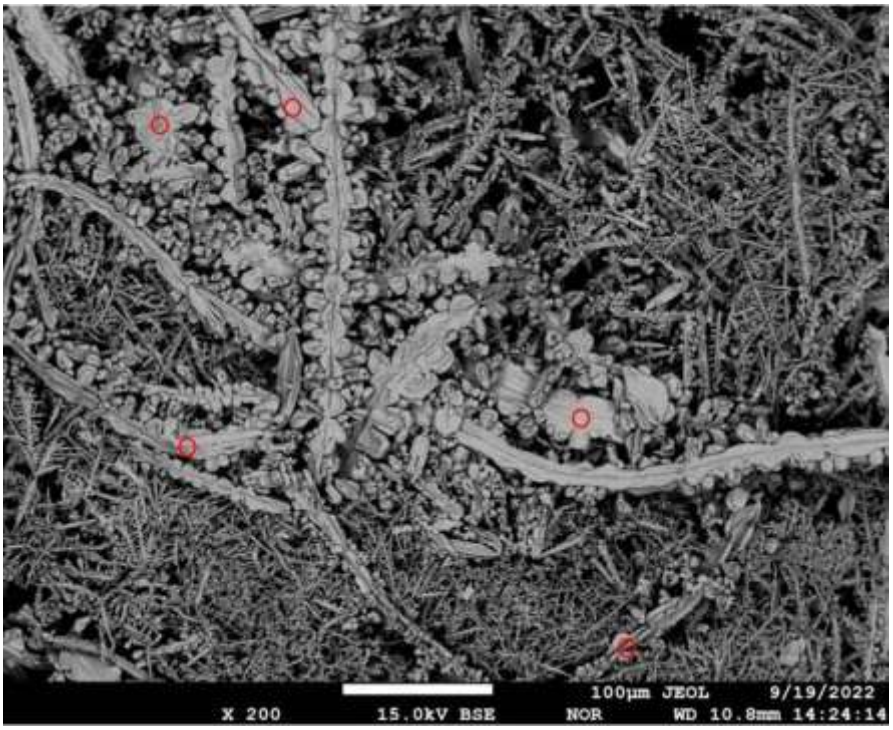

Figure 3-4: SEM Image of the Deposit Formed on the Working Electrode During Electrowinning

Electrowinning of Ag from the fluoride solution was demonstrated with EDS analysis. However, the Ag recovery rate was still comparatively low due to the low molarity of AgF employed. Therefore, two electrowinning conditions: reduction potential and electrowinning time, were experimented with to optimize the Ag percent recovery and determine the coulombic efficiency of the electrowinning process. The following two formulas were used for percent recovery and coulombic efficiency, respectively:

$$CE = \frac{W_F}{W_T} * 100 \quad (4)$$

$$W_T = \frac{MW_{Ag} * I * t}{n * F} \quad (5)$$

Where W_F is the weight of the final deposition (g), W_I is the weight of initial Ag (g), W_T is the theoretical weight of deposition (g), MW_{Ag} is the molecular weight of silver (g/mol), I is the current (A), T is the time (sec), n is the oxidation state (e^- involved in reaction), and F is Faraday's constant (C).

When different potentials between -0.6 V and -1 V were applied for 4 h, a positive correlation between the applied negative potential and the Ag recovery rate was observed in Figure 3-5. An issue arose with -1 V as it yielded a recovery rate of 102.9%. This indicates the possibility of other material or water present in the deposit, which is mostly likely due to a contamination issue, further analyses should be done to confirm the percent recovery.

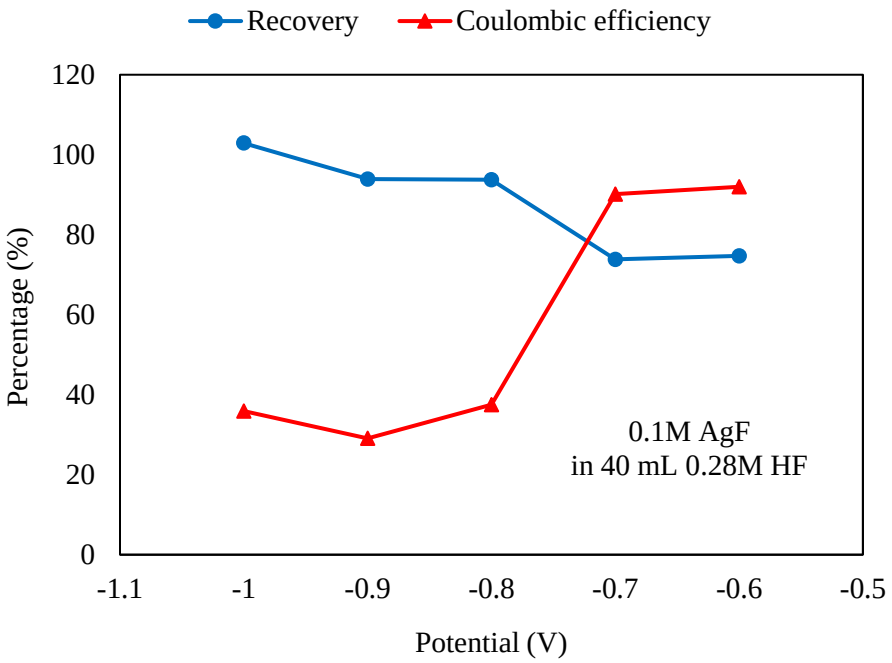

Figure 3-5: Percent Recovery and Coulombic Efficiency of Ag Electrowon as a Function of Potential in 0.28 M AgF in 40 mL of 0.28 M HF

Meanwhile, the trend in coulombic efficiency is the opposite (Figure 3-5). At –0.6 V, the coulombic efficiency after 4 h is 92%, but it drops to around 35% at –0.8 V and –1 V. The low coulombic efficiency suggests a parasitic or competing reaction during Ag electrowinning.

From the experiments in Figure 3-5, a potential of -1 V was chosen to replicate the experiments for different time intervals between 2 h and 24 h, to achieve over 90% Ag recovery. The amount of AgF in the solution was increased to minimize human and experimental errors. Table 3.1 demonstrates the results. Longer duration times result in higher recovery rates. After 24 h, the Ag recovery rate is 95.9%. On the other hand, the coulombic efficiency decreases with longer time, which is consistent with the hypothesis that there is a competing reaction during electrowinning from an AgF solution.

Table 3.1: Ag Recovery Rate and Coulombic Efficiency as a Function of Electrowinning Time at -1 V Versus Ag/AgCl

Time (hour)	Recovery (%)	Coulombic Efficiency (%)
2	33.8	79.4
4	73.9	62.3
8	89.8	48.3
12	95.5	27.8
24	95.9	12.3

From Figure 3-2, there is a sudden drop in current efficiency when electrowinning is run at -0.7 V versus -0.8 V. It would be assumed that at a constant potential, as time elapsed, the trend would follow that seen in Table 3.1. However, the same relationship is seen but the values differ more. The coulombic efficiency is much higher with no values under 50% meanwhile recovery rate lingers around 95%. Even though the potential at -1 V for 24 hours gives the highest recovery, it comes as a tradeoff with coulombic efficiency. The overpotential at -1 V could have caused a parasitic reaction to occur where there is the coevolution of hydrogen on the cathode with oxygen oxidation on the anode. The reason could be due to a surge of current needed due to the depleted ions near the electrode in which the mass transport is limited at the specified current. This in turn causes a higher overpotential to overcome the limited mass transport, which causes unwanted side reactions to occur.

Table 3.2: Ag Recovery Rate and Coulombic Efficiency as a Function of Electrowinning Time at -0.6 V Versus Ag/AgCl

Time (hour)	Recovery (%)	Coulombic Efficiency (%)
4	73.5	93.4
8	89.7	86.1
12	94.9	75.6
24	90.0	64.1

Realistically, values between -0.6 V through -0.8 V should be explored to give high recovery while maximizing current efficiency. Although, the time of the experiments would need to be increased to see if similarly high recovery rates could be achieved as those at -1 V, while still maintaining the coulombic (current) efficiency.

The possibility of a competing reaction is further supported by the current versus time plot below. As the current reaches 0 A, a steady decrease is seen following a steep drop in current. This causes the system to apply a larger overpotential as indicated by the Tafel equation. It would be assumed in this cell that as the silver is depleted from the solution the current being applied should reach towards zero the closer the recovery is to 100%. However, in this cause a large difference is seen in a repetitive sequence as time progresses.

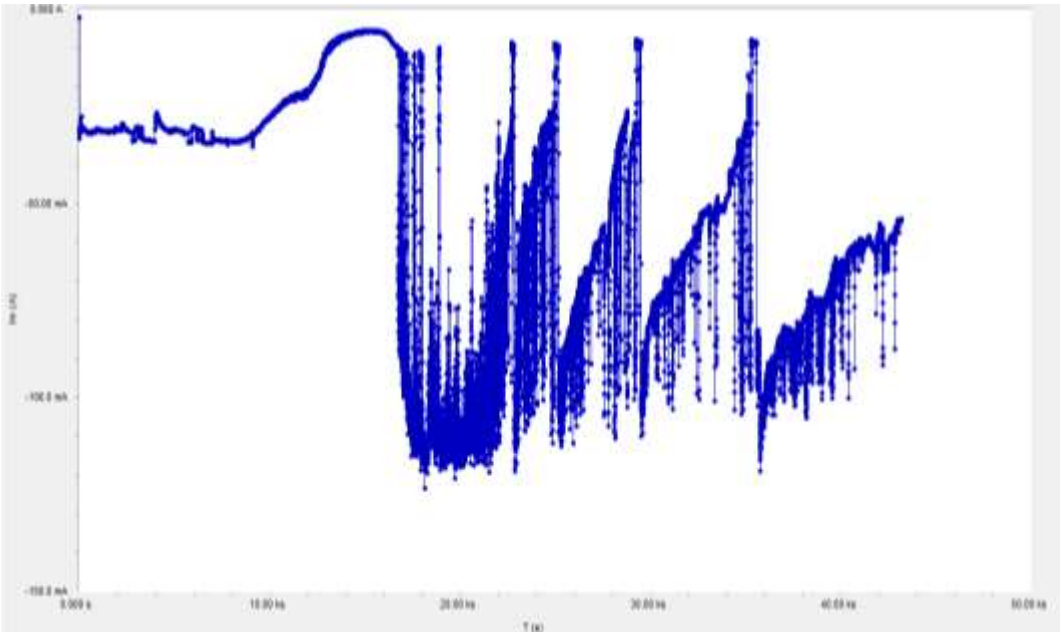

Figure 3-6: Chronoamperometry Scan of Synthetic Electrowinning at -1 V for 12 Hours

Throughout trials and experiments with silver fluoride and HF, different routes were chosen on the working electrode, reference electrode and the system apparatus. It was visible that these processes produced different morphology silver depending on the systems. However, even with the same conditions, time durations and concentrations played a role in morphology.

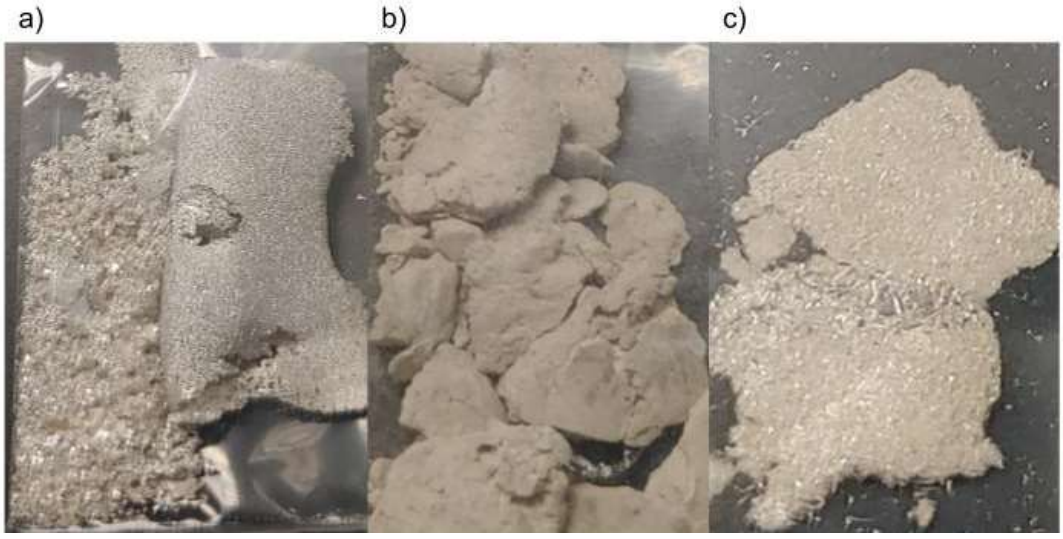

Figure 3-7: Ag Morphology Across Varying Systems in a, b, and c, Respectively

In Figure 3-6a, the system consisted of 0.35M AgF with 40 mL of 1% HF. The electrodes were silver WE, graphite CE and Ag/AgCl RE. The electrowinning ran at -0.2V for 24 hours. Figure 3-6b is vacuum chamber recovered Ag where 0.03M AgF was dissolved in 350 mL 1% HF. The volume of the system was increased due to an apparatus that was created to allow for feeding tubes to create a vacuum seal. The system ran under 34 torr for 24 hours at -0.2V. A change in color and corrosion was seen with the RE, therefore, it is presumed hydrofluoric acid played a role in altering the inside of the 3M potassium chloride solution located between in the RE. Figure 3-6c was with 0.01M AgF with 40

mL 1% HF. This was with graphite WE, CE and RE. With the varying morphologies seen above, EDS confirmed that these are all 100% silver.

3.3 Solar Cell Leaching and Electrowinning

Selective leaching was used to remove components of the solar cell to avoid interference during silver leaching and electrowinning. The corresponding steps are displayed in the figure below. From Figure 3-7a, the back of the solar cell indicates areas that are shinier in which aluminum has been leached. In Figure 3-7b, the blue color is no longer visible from the front and back, it shows a depletion of the silicon nitride layer. Both chemicals were properly disposed of before conducting the experiment in Figure 3-7c where silver was leached using hydrofluoric acid and hydrogen peroxide. Located in the right-hand upper corner, a film of grey can be seen floating near the top of the solution. In the same image, indicated by the red circle is a silver contact located on the back of the cell that is still visible. The resulting solution after the leaching of silver was used for electrowinning.

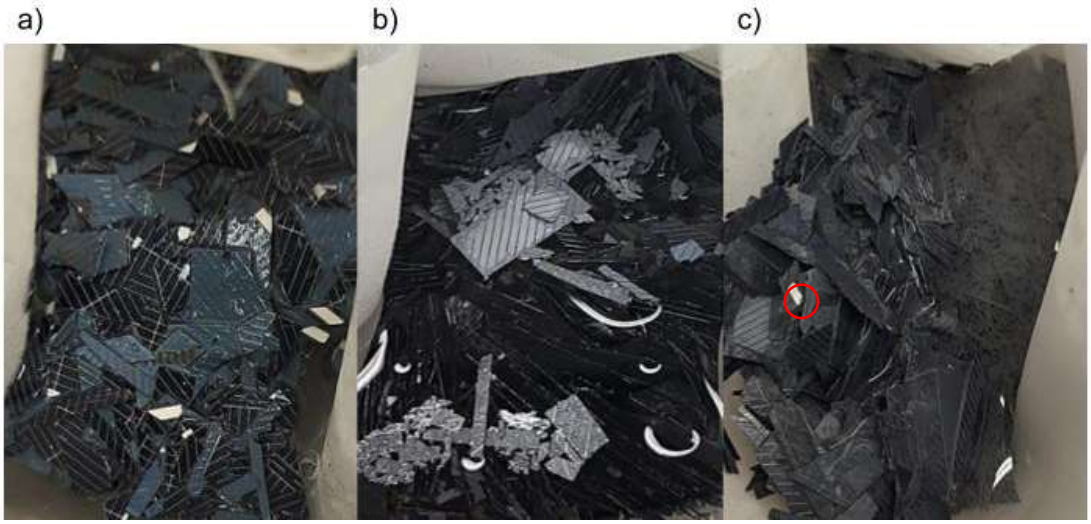

Figure 3-8: Leaching for Removal of a) aluminum, b) Si-N_x layer, and c) silver

It is important to note that before electrowinning, there consisted of a purple deposit that remained from silver leaching (Appendix D). This deposit should have been filtered before electrowinning to remove the visible impurity.

Below is the result from 24 hours of electrowinning the 10 Al-BSF cells. It is composed of two parts, in the red is the silver around the working electrode and the silver that is deposited on the bottom surface. The material was porous but once dried resulted in visibly less silver.

Figure 3-9: Electrowon Silver from Solar Cells with the Silver Located Around the WE and the Bottom

From Figure 3-10, the two components were analyzed using EDS to confirm that both the working electrode was 100% silver. Whereas, the bottom of the container contained trace amounts of silicon, making the silver 99.87% pure Ag.

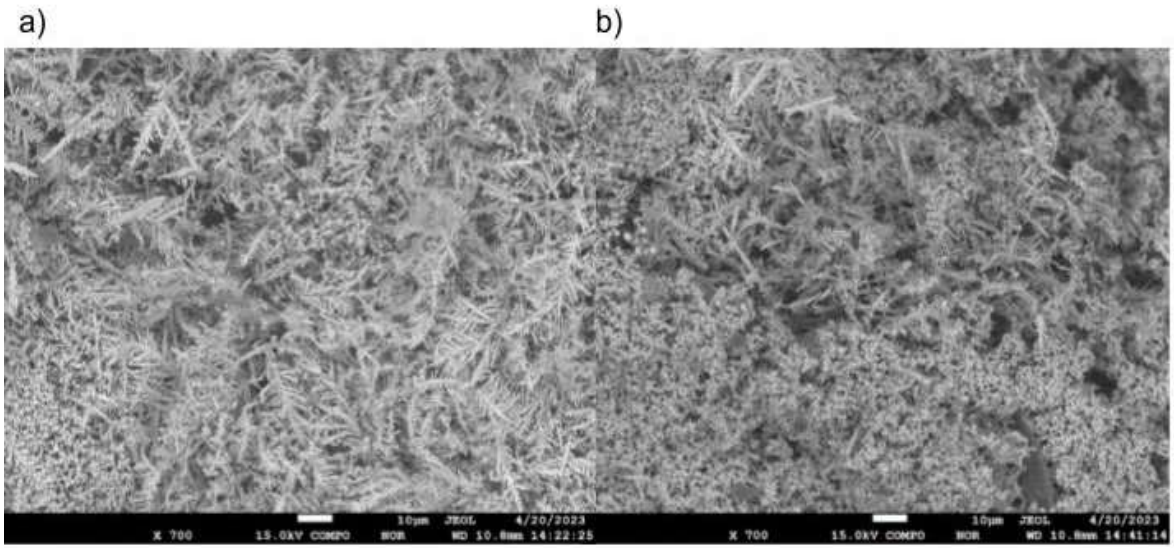

Figure 3-10: Silver from Solar Cells Deposited on the a) Working Electrode and b) Bottom of the Container

For the process of electrowinning silver, the assumption of approximately 0.1 g of silver was in each solar cell. For 10 cells, that would equate to around 1 g of silver that can be recovered. The recovery rate of the silver from the solar cells was around 30%. It is hypothesized that silicon may have been reacting with silver, HF, and peroxide to etch the silicon. This is further visible by the deposit that was formed after leaching silver and the silver that was still present on the cell upon electrowinning. For this system, the nature of HF does not allow for the leaching solution to be analyzed through ICP-MS from its reactivity with glass and its detection limit of Ag even when diluted.

It was hypothesized that silicon dissolution was present in the leached solution (depicted in Figure 3-8c). Chartier et al. [35] conducts a study on the metal-assisted chemical etching (MACE) of silicon in etc. In this study, Ag nanoparticles are used as a catalyst for this process. Instead of the HF and hydrogen peroxide dissolving silver, the hydrogen peroxide also causes etching to occur with the silicon that is further aided by the presence

of silver. Depending on the penetration rate, 3 different formations could develop: pore, crater or polishing. The most likely out of these three would be polishing regime due to the low HF and higher H_2O_2 concentration which is signified by a silicon oxide layer (presence of oxygen) seen in Table 3.3.

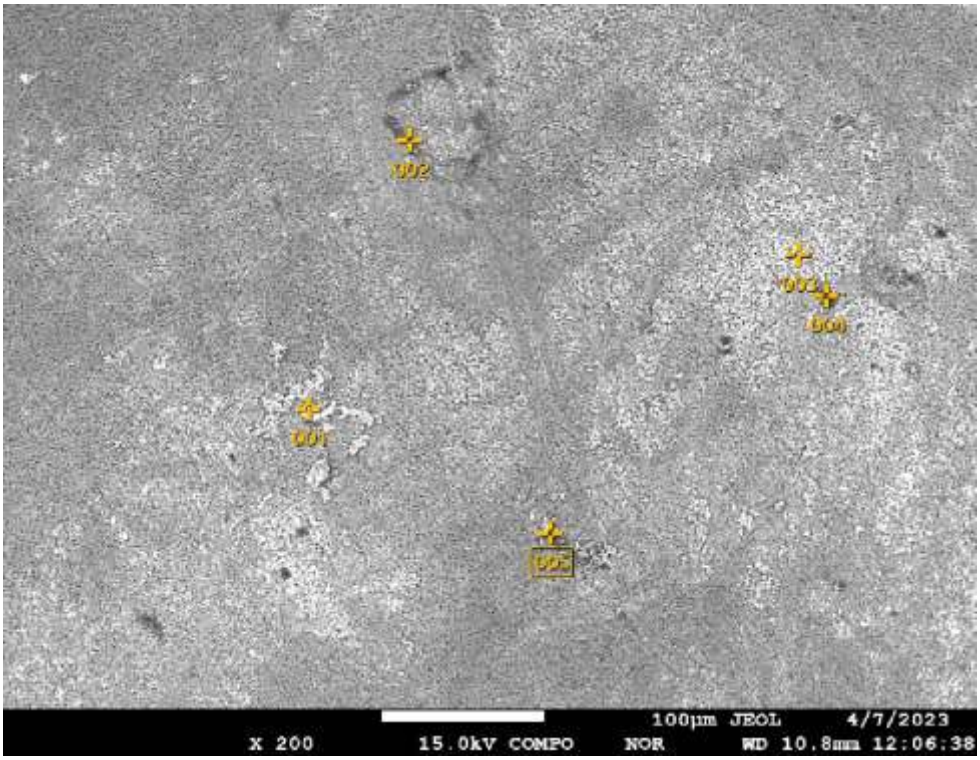

Figure 3-11: HF and Peroxide Leaching on a Solar Cell

Table 3.3: Corresponding Analysis for Figure 3-11 of Elemental Constituents

	O	**Na**	**Al**	**Si**	**Ca**	**Ag**
001	24.42			34.91		40.67
002	34.53	0.43	1.78	62.87	0.40	
003	7.48			82.59		9.93
004	15.34			53.43	9.05	22.19
005	35.96		0.41	17.19	23.46	22.98
Average	23.54	0.43	1.09	50.20	10.97	23.94
Deviation	12.26	0.00	0.97	25.22	11.65	12.65

The presence of silicon in the solution could present further problems during electrowinning. The stability constant (β) was examined for the possible formations in the solution of AgF and SiF_6. The stability constant is the tendency for a complex to be formed. The higher the value indicates that the interaction between the reagents form strong bonds and interactions. For the silver fluoride system, a very weak complex formation was seen of 0.4 ± 0.2 l*mol^{-1} [36]. Whereas the value of $1.5*10^{30} \pm 0.6$ l*mol^{-1} for SiF_6 [37]. Values for varying subscripts of fluorine were tested but only SiF_6 yielded in values that were large enough for complexing. This could mean that a silicon fluoride system could not have been as favorable as silver fluoride. In the chance that silicon fluoride formed, this could cause the migration of AgF to be more challenging, thus decreasing the transport rate and could contribute to the low recovery of 30%.

CHAPTER 4 CONCLUSION AND FUTURE WORK

A fluoride chemistry is proposed for Ag recovery from silicon solar cells involving leaching and electrowinning. Ag leaching requires two chemicals: HF and H_2O_2, and complete Ag dissolution can be achieved within an hour given a 1:2 molar ratio of Ag to H_2O_2 with excess HF. The reduction potential of Ag in a 0.05 M AgF solution is –0.41 V versus Ag/AgCl. Experiments with different reduction potentials and time intervals indicate that there is a reverse correlation between Ag recovery rate and coulombic efficiency during the electrowinning process. The percent recovery values corresponding to -0.6 V demonstrate that values are slightly lower than those at -1 V. The highest Ag recovery rate achieved is over 95% with a reduction potential of -1 V for 24 h. EDS confirms that the deposit on the working electrode after electrowinning is 100% pure Ag. However, the largest difference lies in the coulombic efficiency. The values at -0.6 V show that over 50% efficiency can be achieved for all trials. However, for -1 V a tradeoff with coulombic efficiency can be attributed to a competing reaction with the coevolution of hydrogen and the oxygen reaction that occurs on the anode. Further experiments should be conducted to determine whether electrowinning time plays a significant role in coulombic efficiency and if the same or higher silver recovery can be achieved at lower potentials while preserving the coulombic efficiency.

A sequential leaching process was conducted to remove aluminum, the silicon nitride layer and silver, respectively. When the same steps as the synthetic solution was conducted, the addition of silicon from the cells posed an issue with the dissolution of silver. It is presumed that silicon interacts in the system. Instead of the hydrofluoric acid

and hydrogen peroxide dissolving silver, the silver acted as a catalyst to etch the silicon. This raises concerns about the limited electrolyte ions and hydrogen peroxide needed for the dissolution of silver. The silicon in the electrowinning solution could cause slower mass transport by bonding to the fluorine ions. However, another scenario to consider is the unoptimized conditions of the scaled-up system. The system included different distances between the electrodes, electrode submergence and solution volume. This alters the reduction peak and kinetics compared to that in a synthetic solution. This could have contributed to the low recovery of 30%. The demonstration that high purity silver (>99%) can be recovered from solar cells was confirmed. A disadvantage of silicon ions in the solution is the regenerative chemistry is not possible unless silicon can be removed from the solution.

For future projects, the proposed process should be conducted with solar cells before testing other parameters to determine if other unwanted reactions occur. A factor that can be investigated is how additives or overpotential affect the surface of the cathode and its deposit to ensure that the deposited surface morphology does not hinder the silver deposition. Additionally, stirring could be employed to help overcome diffusion-limited transport especially when there are low concentrations of the silver ions. Another option for the HF system is to recover the silver using additional processing or refining steps such as precipitation. The exploration of the electrolyte methanesulfonic acid (MSA) poses as a good substitution of hydrofluoric acid due to its milder chemistry and environmental advantage.

REFERENCES

[1] A Paiano, “Photovoltaic waste assessment in Italy,” Renewable and Sustainable Energy Reviews, vol. 41, pp. 99–112, Jan. 2015.

[2] “End-of-Life Management for Solar Photovoltaics.” Office of Energy Efficiency and Renewable Energy, www.energy.gov. Accessed May 2023.

[3] I. Kaizuka, R. Kurihara, H. Matsukawa, G. Masson, S. Nowak, and M. Brunisholz, “Trends 2015 in Photovoltaic Applications,” IEA International Energy Agency, 2015. [Online]. Available: https://iea-pvps.org/wp-content/uploads/2020/01/IEA-PVPS_-_Trends_2015_-_MedRes.pdf.

[4] C. C. Farrell, A. I. Osman, R. Doherty, M. Saad, X. Zhang, A. Murphy, J. Harrison, A. S. M. Vennard, V. Kumaravel, A. H. Al-Muhtaseb, and D. W. Rooney, “Technical challenges and opportunities in realising a circular economy for waste photovoltaic modules,” Renewable and Sustainable Energy Reviews, vol. 128, Aug. 2020.

[5] Azevedo, M, et al. “The Raw-Materials Challenge: How the Metals and Mining Sector Will Be at the Core of Enabling the Energy Transition.” McKinsey & Company, McKinsey & Company, 10 Jan. 2022, www.mckinsey.com/industries/metals-and-mining/our-insights/the-raw-materials-challenge-how-the-metals-and-mining-sector-will-be-at-the-core-of-enabling-the-energy-transition.

[6] IRENA. “End-of-Life Management Solar Photovoltaic Panels.” End-of-Life Management Solar Photovoltaic Panels, 1 June 2016, www.irena.org/publications/2016/Jun/End-of-life-management-Solar-Photovoltaic-Panels.

[7] V. M. Fthenakis, “End-of-life management and recycling of PV modules,” Energy Policy, vol. 28, no. 14, pp. 1051–1058, 2000.

[8] X. Wang, X. Tian, X. Chen, L. Ren, and C. Geng, “A review of end-of-life crystalline silicon solar photovoltaic panel recycling technology,” Solar Energy Materials and Solar Cells, vol. 248, 2022.

[9] C. Modrzynski, L. Blaesing, S. Hippmann, M. Bertau, J. Z. Bloh, and C. Weidlich, “Electrochemical recycling of photovoltaic modules to recover metals and silicon wafers,” Chemie Ingenieur Technik, vol. 93, no. 11, pp. 1851–1858, 2021.

[10] M. Tao, V. Fthenakis, B. Ebin, B. M. Steenari, E. Butler, P. Sinha, R. Corkish, K. Wambach, and E. S. Simon, “Major challenges and opportunities in Silicon Solar

Module Recycling," Progress in Photovoltaics: Research and Applications, vol. 28, no. 10, pp. 1077–1088, 2020.

[11] Peplow, Mark. "Solar Panels Face Recycling Challenge." C&En, 22 May 2022, cen.acs.org/environment/recycling/Solar-panels-face-recycling-challenge-photovoltaic-waste/100/i18.

[12] Wollschlaeger, Sara. "Leaching in Metallurgy and Metal Recovery." Emew Blog, Emew Corporation, 10 July 2017, blog.emew.com/leaching-in-metallurgy-and-metal-recovery.

[13] "23.3: Hydrometallurgy." Chemistry LibreTexts, Libretexts, 8 Sept. 2020, chem.libretexts.org/Courses/University_of_Missouri/MU%3A__1330H_(Keller)/23%3A_Metals_and_Metallurgy/23.3%3A_Hydrometallurgy#:~:text=Hydrometallurgy%20involves%20the%20use%20of,metals%20like%20gold%20and%20silver.

[14] Admin. "Leaching Process - Chemistry of Extracting Substances via Leaching." BYJUS, 22 July 2022, byjus.com/chemistry/leaching-process/.

[15] Richardson, J.F., et al. "Leaching." Chemical Engineering, 2002, pp. 502–541, https://doi.org/10.1016/b978-0-08-049064-9.50021-7.

[16] Jorge. "Electrowinning." Metallurgist & Mineral Processing Engineer, 17 Nov. 2020, www.911metallurgist.com/electrowinning/.

[17] Barshai, Alex. "Electrowinning 101: What Is Electrowinning?" Emew Blog, Emew Corporation, 13 Dec. 2022, blog.emew.com/electrowinning-101-what-is-electrowinning.

[18] Bard, Allen J., et al. *Electrochemical Methods: Fundamentals and Applications*. Wiley, 2022.

[19] Wang, W., et al. "Electrochemical cells for medium- and large-scale energy storage." Advances in Batteries for Medium and Large-Scale Energy Storage, 2015, pp. 3–28, https://doi.org/10.1016/b978-1-78242-013-2.00001-7.

[20] Werner, J. M., et al. "Editors' choice—modeling and validation of local electrowinning electrode current density using two phase flow and Nernst–Planck equations." Journal of The Electrochemical Society, vol. 165, no. 5, 31 Mar. 2018, https://doi.org/10.1149/2.0581805jes.

[21] Elgrishi, Noémie, et al. "A practical beginner's guide to cyclic voltammetry." Journal of Chemical Education, vol. 95, no. 2, 2017, pp. 197–206, https://doi.org/10.1021/acs.jchemed.7b00361.

[22] “Nernst Equation.” Chemistry LibreTexts, Libretexts, 29 Aug. 2023, chem.libretexts.org/Bookshelves/Analytical_Chemistry/Supplemental_Modules_(Analytical_Chemistry)/Electrochemistry/Nernst_Equation.

[23] Leslie, Nathaniel, and Janine Mauzeroll. “Spatially resolved electrochemical measurements.” Encyclopedia of Solid-Liquid Interfaces, 2024, pp. 461–478, https://doi.org/10.1016/b978-0-323-85669-0.00004-0.

[24] Vanysek, Petr. Modern Techniques in Electroanalysis. Wiley, 1996.

[25] “Silver - Element Information, Properties and Uses: Periodic Table.” Silver - Element Information, Properties and Uses | Periodic Table, www.rsc.org/periodic-table/element/47/silver. Accessed Dec. 2023.

[26] Admin. “Reactivity Series - Reactivity Series of Metals Chart, Features, Uses.” BYJUS, BYJU’S, 27 Sept. 2023, byjus.com/chemistry/reactivity-series/.

[27] “CDC.” Centers for Disease Control and Prevention, Centers for Disease Control and Prevention, 4 Apr. 2018, emergency.cdc.gov/agent/hydrofluoricacid/basics/facts.asp.

[28] “Hydrogen Fluoride.” ICSC 0283 - Hydrogen Fluoride, Apr. 2017, www.inchem.org/documents/icsc/icsc/eics0283.htm.

[29] “Silver Mining and Refining.” Education, Education, 28 Jan. 2018, www.thenaturalsapphirecompany.com/education/precious-metal-mining-refining-techniques/silver-mining-refining/.

[30] Drif, Boujemaa, et al. “Recovery of residual silver-bearing minerals from low-grade tailings by froth flotation: The case of Zgounder Mine, Morocco.” Minerals, vol. 8, no. 7, 2018, p. 273, https://doi.org/10.3390/min8070273.

[31] “Sodium Cyanide: Systemic Agent.” Centers for Disease Control and Prevention, Centers for Disease Control and Prevention, 12 May 2011, www.cdc.gov/niosh/ershdb/emergencyresponsecard_29750036.html.

[32] Dias, P.; Javimczik, S.; Benevit, M.; Veit, H.; Bernardes, A. M. Recycling Weee: Extraction and Concentration of Silver from Waste Crystalline Silicon Photovoltaic Modules. Waste Management 2016, 57, 220–225. DOI:10.1016/j.wasman.2016.03.016.

[33] Oliveira, L. S.; Lima, M. T.; Yamane, L.; Siman, R. R. Silver Recovery from End-of-Life Photovoltaic Panels. Detritus 2020, No. 10, 62–74. DOI:10.31025/2611-4135/2020.13939.

[34] Yang, E.-H.; Lee, J.-K.; Lee, J.-S.; Ahn, Y.-S.; Kang, G.-H.; Cho, C.-H. Environmentally Friendly Recovery of AG from End-of-Life C-Si Solar Cell Using Organic Acid and Its Electrochemical Purification. *Hydrometallurgy* **2017**, *167*, 129–133. DOI:10.1016/j.hydromet.2016.11.005.

[35] Chartier, C., et al. “Metal-assisted chemical etching of silicon in Hf–H2O2.” Electrochimica Acta, vol. 53, no. 17, July 2008, pp. 5509–5516, https://doi.org/10.1016/j.electacta.2008.03.009.

[36] Singh, Jagvir, et al. “Stability constants of metal complexes in solution.” Stability and Applications of Coordination Compounds, 2020, https://doi.org/10.5772/intechopen.90183.

[37] Roberson, C.E., and Roberta B. Barnes. “Stability of fluoride complex with silica and its distribution in natural water systems.” Chemical Geology, vol. 21, no. 3–4, Feb. 1978, pp. 239–256, https://doi.org/10.1016/0009-2541(78)90047-5.

APPENDIX A

CYCLIC VOLTAMMOGRAMS FOR GRAPHITE WE, CE, AND RE OF 1% HF SOLUTION

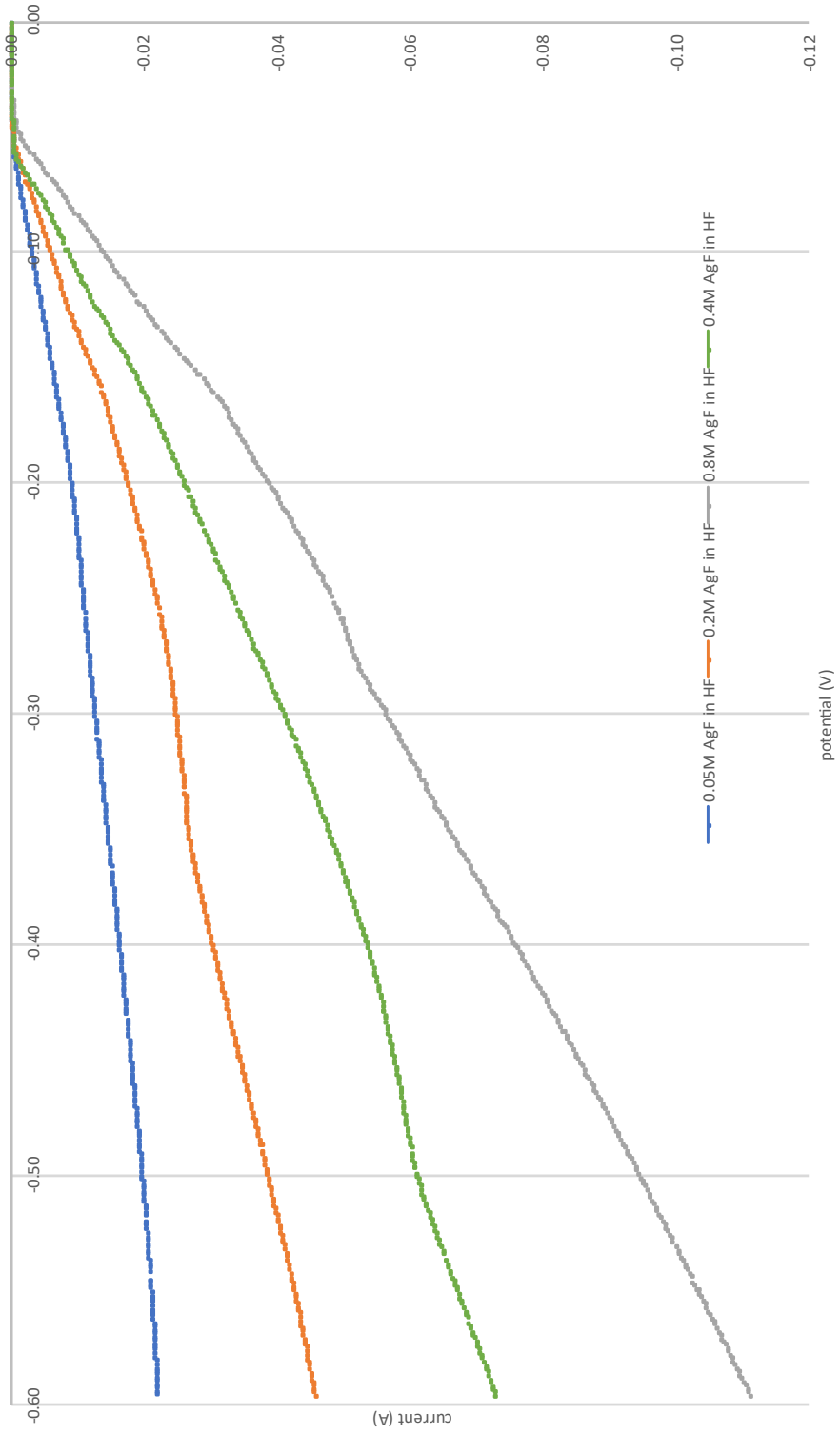
0.00
-0.02
-0.04
-0.06
-0.08
-0.10
-0.12
0.00
-0.10
-0.20
-0.30
-0.40
-0.50
-0.60
current (A)
potential (V)
0.05M AgF in HF
0.2M AgF in HF
0.8M AgF in HF
0.4M AgF in HF

APPENDIX B
EXPERIMENTAL CONDITIONS TESTED WITH GRAPHITE WE AND CE

Electrowinning conditions	Initial Ag (g)	Recovery (%)	Current Efficiency (%)
-0.6V, 4 hrs	0.431927	74.71169897	91.9859288
-0.8V, 4 hrs	0.431927	93.71954057	37.51056186
-1V, 4 hrs	0.431161775	102.8848163	35.94163552
-1V, 8 hrs	0.43107675	96.75771194	14.08956486
-1V, 12 hrs	0.4312468	92.87025434	15.76774418
-0.6V, 4 hrs	0.431331825	73.51648583	93.42644991
-1V, 11 hrs	0.431501875	88.8061031	10.11414797
-1V, 24 hrs	0.43107675	97.22166644	4.271170755
-0.6V, 24 hrs	0.430651625	88.95821536	64.1120722
-0.6V, 8 hrs	0.430991725	89.74650267	86.08824035
-0.6V, 12 hrs	0.43141685	94.89661797	75.61513659
-0.7V, 4 hrs	0.431331825	73.84106192	90.18518126

APPENDIX C
SEM IMAGES OF VARYING MORPHOLOGY SILVER CORRESPONDING TO FIGURE 3-7

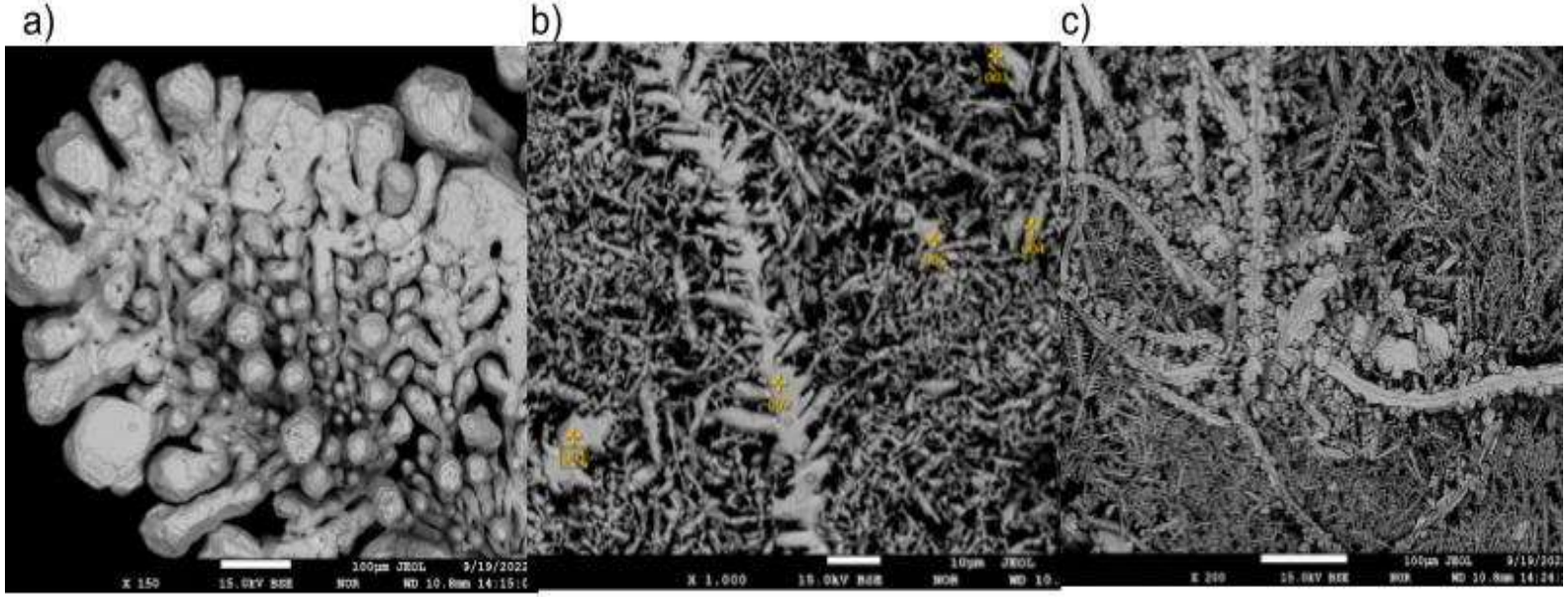
a)
b)
c)

APPENDIX D

SOLAR CELL LEACHING PURPLE DEPOSIT